ISSN 0010-9525, Cosmic Research, 2024, Vol. 62, No. 4, pp. 330–338. © Pleiades Publishing, Ltd., 2024.

ELVES Measurements in the "UV Atmosphere" (Mini-EUSO) Experiment Onboard the *ISS* and Their Reconstruction

S. Sharakin[a, *], D. Barghini[b–d], M. Battisti[b, e], A. Belov[a, f], M. Bertaina[b, c], M. Bianciotto[b, c], F. Bisconti[g], C. Blaksley[h], S. Blin[e], G. Cambiè[g, i], F. Capel[j], M. Casolino[g, h, i], T. Ebisuzaki[h], J. Eser[k], F. Fenu[l], M. A. Franceschi[m], A. Golzio[b, c], P. Gorodetsky[e], F. Kajino[n], H. Kasuga[h], P. Klimov[a], M. Manfrin[b, c], L. Marcelli[i, g], W. Marszal[o], H. Miyamoto[b, c], M. Mignone[b], A. Murashov[a], T. Napolitano[m], H. Ohmori[h], A. Olinto[k], E. Parizot[e], P. Picozza[g, i], L. W. Piotrowski[p], Z. Plebaniak[g, i], G. Prévôt[e], E. Reali[g, i], M. Ricci[m], G. Romoli[g, i], N. Sakaki[h], K. Shinozaki[o], J. Szabelski[q], C. De La Taille[r], Y. Takizawa[h], M. Vrábel[o], L. Wiencke[s], and M. Zotov[a]

[a] *Skobeltsyn Institute of Nuclear Physics, Moscow State University, Moscow, 119991 Russia*
[b] *INFN Section of Turin, Turin, 10125 Italy*
[c] *Department of Physics, University of Turin, Turin, 10125 Italy*
[d] *INAF Astrophysics Observatory of Turin, Pino Torinese, 10025 Italy*
[e] *Université Paris Cité, CNRS, Astroparticule et Cosmologie, Paris, 75013 France*
[f] *Faculty of Physics, Moscow State University, Moscow, 119991 Russia*
[g] *INFN Section of Rome Tor Vergata, Rome, 00133 Italy*
[h] *RIKEN, Wako, 351-0198 Japan*
[i] *Department of Physics, University of Rome Tor Vergata, Rome, 00133 Italy*
[j] *Technical University of Munich, Munich, 80333 Germany*
[k] *Department of Astronomy and Astrophysics, The University of Chicago, Chicago, IL 60637 United States*
[l] *Agenzia Spaziale Italiana, Roma, 00133 Italy*
[m] *INFN National Laboratories of Frascati, Frascati, 00044 Italy*
[n] *Department of Physics, Konan University, Kobe, Hyogo, 658-8501 Japan*
[o] *National Centre for Nuclear Research, Otwock, 05-400 Poland*
[p] *Faculty of Physics, University of Warsaw, Warsaw, 02-093 Poland*
[q] *Stefan Batory Academy of Applied Sciences, Skierniewice, 96-100 Poland*
[r] *Omega, Ecole Polytechnique, CNRS/IN2P3, Palaiseau, 91120 France*
[s] *Department of Physics, Colorado School of Mines, Golden, CO 80401 United States*
**e-mail: sharakin@mail.ru*

Received August 16, 2023; revised September 9, 2023; accepted September 11, 2023

Abstract—More than three dozen submillisecond events of ELVES type ("elves"), which are the result of the interaction of the front of an electromagnetic pulse from a lightning discharge and the lower layer of the ionosphere, have been identified in the data of a UV Atmosphere orbital multichannel detector (Mini-EUSO). Each event has a characteristic annular glow pattern and occupies a significant part of the detector's field of view, and the signal in a separate channel has an asymmetric profile with a pronounced peak. The distribution of peak times contains information about both the localization of the discharge and the altitude of the glow. In this paper, we propose a Bayesian (probabilistic) model for reconstructing ELVES events, implemented using probabilistic programming methods in PyMC-5. The capabilities of the model for determining the position of the discharge are shown using the example of several events. Methods for modifying the model to restore the discharge orientation and refine the glow height are outlined.

Keywords: UV atmosphere, orbital detector, transient atmospheric phenomena, Bayesian inference, probabilistic programming

DOI: 10.1134/S0010952524600379

INTRODUCTION

Since autumn 2019, the UV Atmosphere detector (Mini-EUSO) [1–3] has been operating in near-Earth orbit. This is an important stage of the scientific program of the international collaboration JEM-EUSO,[1] which is aimed at studying cosmic rays of extremely high energies. The detector is attached to the inner side of the UV-transparent window of the

[1] Joint Exploratory Missions for an Extreme Universe Space Observatory.

Russian module Zvezda of the *International Space Station* (*ISS*) and is oriented (approximately) at nadir. It is a lens telescope (25-cm entrance pupil diameter, 30-cm focal length), with a photodetector consisting of 36 multianode photomultiplier tubes (MAPMTs) installed at its focus. The photodetector has 2304 highly sensitive channels covering an area of 100000 km^2 with a temporal resolution of 2.5 μs. In addition to the main mode of recording data with a trigger, continuous monitoring with a temporal resolution of 41 ms is carried out in parallel. The spectral sensitivity of the instrument is determined by the characteristics of the photocathode and the BG3 filter and is in the near UV range (300–400 nm). More details about the instrument and its characteristics can be found in [4, 5], and its trigger is described in [6, 7].

The wide field of view and high temporal resolution and sensitivity make Mini-EUSO particularly effective for studying various types of transient luminous events (TLEs) in the upper atmosphere [8, 9]. One of the most common types of TLEs is called ELVES,[2] which are sub-millisecond flashes in the form of rapidly expanding rings at an altitude of about 90 km. These are often simply called "elves", perhaps because of their fleeting and elusive nature (but with singular "elve").

The occurrence of elves is associated with the influence of a powerful electromagnetic pulse (EMP) from lightning discharge on the lower layers of the ionosphere [10, 11], resulting in a noticeable increase in electron density, their heating, and ionization of air molecules at altitudes of 85–95 km. The region of increased ionization is localized in altitude and propagates according to the expansion of the spherical front of the EMP. Luminescence in the lines of the first negative and second positive nitrogen systems leads to the observed "superluminous" growth of the elve ring [12].

Elves have been observed multiple times both from the ground (see, e.g., [11, 13]) and from space starting from random photographs from the Space Shuttle [14] and ending with systematic measurements using ISUAL [15] and TUS [16, 17] detectors. The results of the ISUAL work indicate [18] that elves are the most common class of TLEs. Registering elves with the Mini-EUSO detector is the next important step in studying them, a phenomenon that is interesting not only in itself (as it relatively new and still poorly understood), but also for the purposes of refining various processes occurring both inside a thundercloud and in the lower layer of the ionosphere [19, 20].

ELVES events are sought for in Mini-EUSO data obtained against the background of thunderstorm activity. Despite the complexity of isolating the pattern of active[3] signals in such conditions, more than 30 elves have been detected to date [21]. A preliminary but detailed analysis of most of these events is presented in [9, 22]. This paper provides a very promising approach to the reconstruction of such events (and some results of its application) based on Bayesian inference and probabilistic programming is provided.

ELVES IN MINI-EUSO

The optics of the Mini-EUSO detector constructs a dynamic image of the elve (located hundreds of kilometers away from the *ISS*), updating it every gate time unit (GTU) = 2.5 μs. In the detector's field of view, only a part of the luminous ring is often captured, and the duration of the event ranges from 100 to 400 μs, i.e., from a few tens to one or two hundred GTUs. The field of view of an individual photodetector channel at an altitude of 90 km is 4.7 × 4.7 km, and hundreds of channels are involved in forming the dynamic image of a typical elve.

Several "instantaneous photographs" of one of the detected events are shown in Fig. 1. The field of view of each of the 2304 channels ("pixels") is projected onto an altitude of 90 km. A group of 64 pixels corresponds to one MAPMT, and horizontal and vertical white stripes represent constructive "dead zones" between adjacent MAPMTs (four MAPMTs in the top right corner of the figure were operating in a reduced sensitivity mode at that moment). Each image is obtained by subtracting the background (using the median value of the signal in the channel immediately before the elve development) with a different time delay in different directions—only in this case does the image pattern have the shape of a annular ring. The width of the ring is associated with both the profile of the current pulse (the elve-generating lightning discharge) and the characteristics of the interaction of EMP with the lower layer of the ionosphere, as well as with the size and shape of the point spread function (PSF) of the detector's optical system. The luminosity intensity (presented in photons per GTU on the vertical scale on the right side of Fig. 1) rapidly decreases as the ring expands, determining the overall duration of the registered event; for the event depicted in the figure, it was approximately 380 μs.

Figure 2 shows the signal of an elve in an individual channel, or more precisely, the signals of two diagonally adjacent channels with numbers (36.14) and (37.13) (the column–row numbering starts from the bottom left corner of the photodetector)—i.e., approximately along the movement of the elve ring. A characteristic asymmetric profile with rapid rise and relatively slower decay is clearly visible in both signals. Such similarity in signals is observed in almost all active channels, allowing the use of the same parametric function for their approximation. In this study, two variants of asymmetric profiles were used: a bi-Gaussian function (merging two Gaussians of different widths at the common maximum) and a Gaussian-exponential profile. The peak position of the signal in time

[2] Emission of Light and Very low frequency perturbations due to Electromagnetic pulse Sources.

[3] We will call "active" both the channels in which the elve signal is detected and these signals themselves, i.e., the characteristic excess of the signal above background.

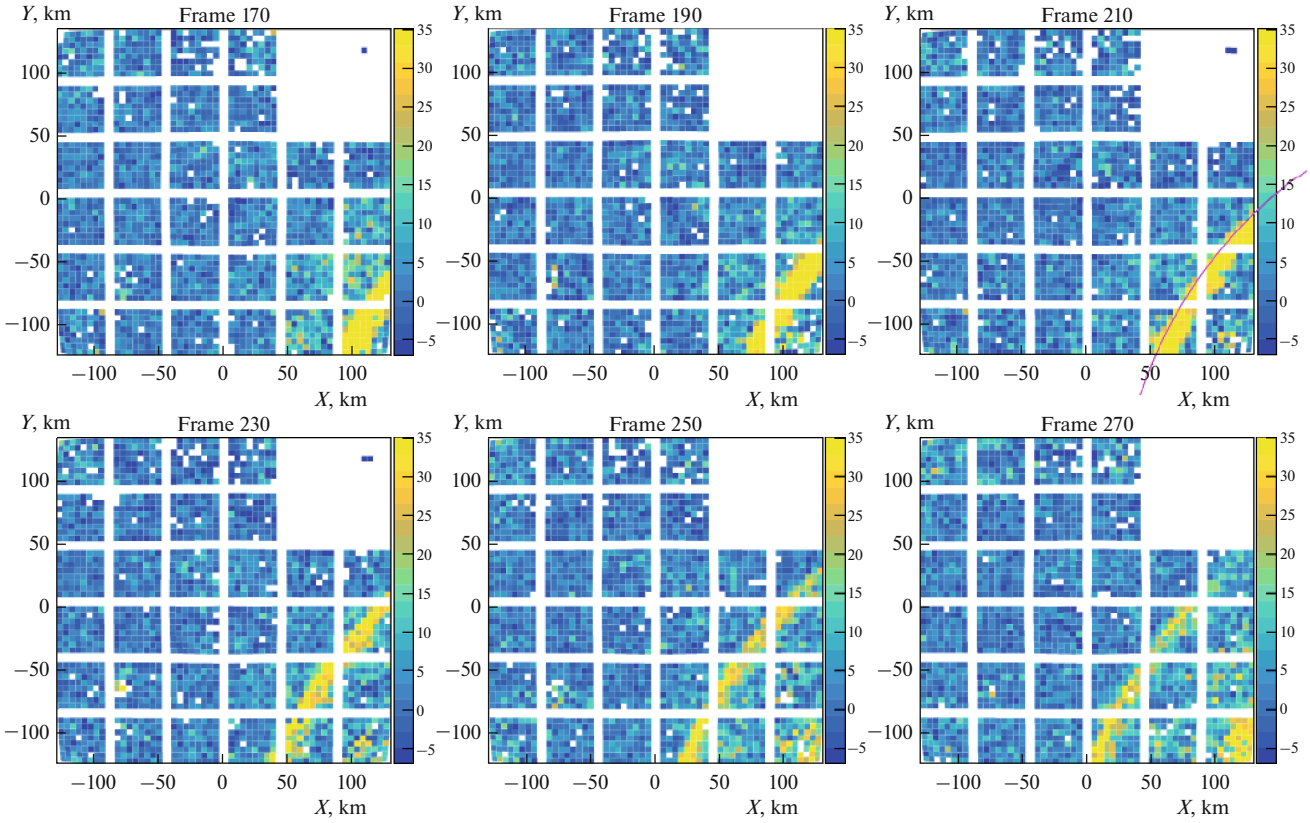

Fig. 1. ELVES event detected on May 12, 2019. Six instantaneous images (projections onto an altitude of 90 km) are provided with an interval of 10 GTU = 25 μs. The result of the current front reconstruction is depicted by the pink line on frame 210.

depends on the channel's position on the photodetector, i.e., the spatial region of the elve viewed by that channel. For example, if the peak position of the signal is determined by the bi-Gaussian profile, the time delay for the two depicted signals is 20.6 μs, while the distance between the centers of the field of view of the channels will be 6.6 km (at an altitude of 90 km).

From a kinematic point of view, the time delay is associated with the difference in the distance traveled by the EMP from the source S (lightning discharge) to the luminous region in the atmosphere. Assuming that the peak of luminosity corresponds to emission from the same level in the atmosphere H_e (elve's altitude), delay Δt_{12} is determined by the position of source $S(x_0, y_0, z_0)$ and the fields of view of the channels:

$$c\Delta t_{12} = \sqrt{h_0^2 + (x_1 - x_0)^2 + (y_1 - y_0)^2} - \sqrt{h_0^2 + (x_2 - x_0)^2 + (y_2 - y_0)^2},$$

where $h_0 = H_e - z_0$, $c \approx 0.75$ km/GTU is the speed of light. Here, a Cartesian horizontal coordinate system anchored to the nadir point of the detector was introduced. In this system, the detector is located at point D (0, 0, H_d), height of the *ISS* orbit H_d (≈420 km) is known with good accuracy for each event, and the centers of the fields of view have coordinates (x_1, y_1) and (x_2, y_2) at altitude $z = H_e$, expressed in terms of polar θ and azimuthal φ angles:

$$x_i = (H_d - H_e)\tan\theta_i\cos\varphi_i,$$
$$y_i = (H_d - H_e)\tan\theta_i\sin\varphi_i.$$

Angles θ_i and φ_i, $i = 1, 2$, determine the direction to the center of the field of view of the ith channel and are easily calculated for each channel considering the orientation of the detector.

BAYESIAN MODEL FOR ELVES RECONSTRUCTION

Any reconstruction involves constructing a *parametric model* of the phenomenon (non-parametric models are not considered in this study) and obtaining various quantitative estimates of the parameters based on data. In the case of physical phenomena, the data usually represent the results of a specially planned and conducted experiment. The model may include both a model of the phenomenon itself and a model of the measurement procedure.

In the Bayesian approach, the model is probabilistic: it is defined in the form of probability distributions [23, 24]. The goal of reconstruction in this case is to

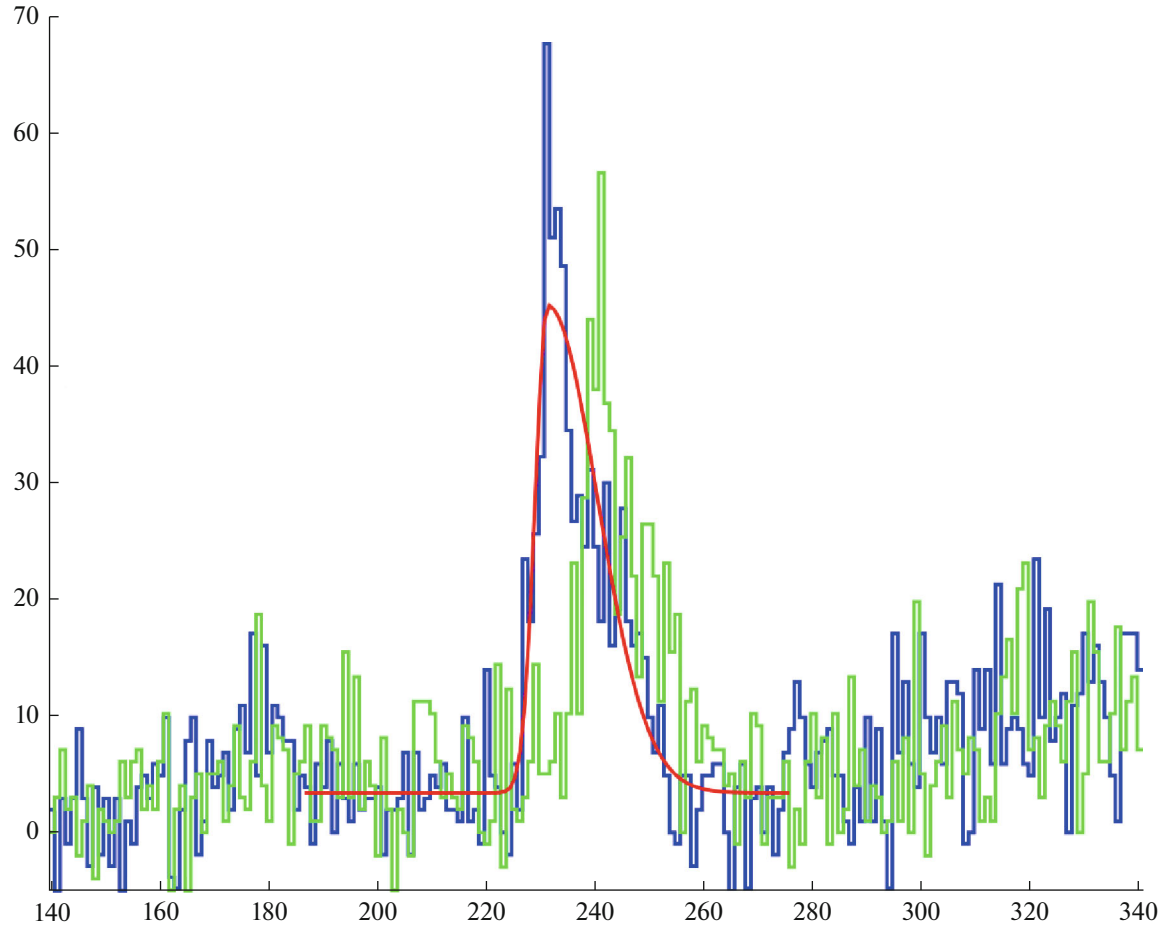

Fig. 2. ELVES20190512 signal in a separate channel (horizontal axis represents time in GTU = 2.5 μs, vertical axis represents signal in photons per GTU). The blue line is channel (37.13), and the green line is channel (36.14). For the first of the signals, an asymmetric profile obtained by approximating with a bi-Gaussian function is shown in red.

obtain the so-called "posterior distribution" for parameters Θ of the model, $p(\Theta|D)$, where D is the experimental data (often preprocessed in some way). To obtain this distribution, it is necessary, based on the available initial information, to specify a prior distribution $p(\Theta)$, formulate a probabilistic measurement model using the likelihood function $p(D|\Theta)$ and use Bayes' theorem:

$$p(\Theta|D) \propto p(\Theta) \times p(D|\Theta).$$

Here, the proportionality constant, which is numerically equal to $1/p(D)$, does not depend on the parameters and only determines the overall normalization of the posterior distribution.

The posterior distribution itself provides exhaustive information about the model parameters. However, it is often more convenient to express the result as a small set of numbers. In this case, the center of the distribution is typically estimated as the mean, and its width is estimated as the standard deviation (square root of the variance). For realistic models, parameter Θ represents a multidimensional quantity, and the results of Bayesian inference can be presented as one-dimensional posterior distributions marginalized over all parameters except one, as well as in the form of pairwise correlation functions.

Sometimes, the set Θ includes parameter(s) η necessary only for formulating the probabilistic model in terms of relatively simple distributions (for example, from the exponential family). Using such auxiliary parameters, marginalization is performed at the end:

$$p(\Theta_0|D) = \int p(\Theta_0, \eta|D)\, d\eta$$
$$\propto \int p(D|\Theta_0, \eta)\, p(\Theta_0)\, p(\eta)\, d\eta$$

(for simplicity, let us assume that the prior factorizes). It should be noted that, in the Bayesian approach, averaging is performed over all values of parameter η, rather than substituting any particular estimate (which would lead to a reduction in the distribution variance).

In recent years, the Bayesian approach has attracted increasing attention [25] due to the development of very efficient (and easy-to-use) samplers, i.e., sampling generators from the posterior distribution,

based on the use of Markov chain Monte Carlo methods such as JAGS,[4] STAN,[5] PyMC,[6] etc. Such approaches have even been named "probabilistic programming." In this work, the probabilistic model (see below) is implemented using the tools of the Python library PyMC-5. Various methods for graphically constructing marginalized distributions were implemented using the ArviZ library (https://www.arviz.org).

In the previous section, the measurements of the elve were projected onto the reference plane $z = H_r = 90$ km, implying that this plane corresponds to the altitude of luminescence ($H_e = H_r$). At the same time, a correction of time was performed: *detector* time T was shifted by an amount determined by the time it takes for the radiation from luminescence area A_i (x_i, y_i, H_r) to reach detector D, $c\Delta T_i = (H_d - H_r)/\cos\theta_i$. If such a correction is not made, and the peak signal times in each active channel, T_i, $i = 1, ..., N$ (N is the number of active channels), are considered as experimental data, then the relationship between the data and the position of the EMP source will be as follows:

$$cT_i = cT_0 + \sqrt{x_i^2 + y_i^2 + (H_d - H_e)^2} + \sqrt{(x_i - x_0)^2 + (y_i - y_0)^2 + (H_e - z_0)^2} + \xi_i.$$

Here, T_0 plays the role of an auxiliary parameter and the last term is the random measurement error of peak time ξ_i.

Thus, it is possible to formulate a probabilistic model defined by the parameters $\Theta \equiv \{x_0, y_0, z_0, T_0, H_e\}$, setting prior distributions on them and refining them (by calculating posterior distributions using Bayes' theorem) with the aid of a set of experimental data $D \equiv \{T_i, \theta_i, \varphi_i\}$. An important step in formulating the model is the choice of the measurement error distribution ξ_i. A reasonable assumption for them would be the condition of independence of their joint distribution (the likelihood function factorizes in this case). Usually, a normal (Gaussian) error model is used (largely for simplicity), but it is not appropriate in our case.

The model construction above implicitly used the assumption that the signal peak corresponds to the passage of the EMP front through the center of the channel's field of view. This hypothesis is justified if the optics of the detector forms a symmetrical image of not very large size. According to the results of calibration tests, the PSF of the telescope has a size of 1.2 pixels and, indeed, does not contain significant asymmetric deviations. However, in the edge pixels, i.e., in the channels located at the boundary of MAPMTs, part of the energy of the instantaneous image falls into the dead zone, and, therefore, there may be a discrepancy between the center of the field and the position of the measured image centroid. It appears impractical to exclude all such channels from the data sample, as in some cases, they constitute a significant part of the entire dataset. One could separately consider such pixels in the sample and assign them an increased measurement error. In this work, the model is made more robust to such deviations by replacing the normal error distribution with a wider distribution. Moreover, to allow the data to determine the characteristic shape of the distribution themselves, a Student's distribution (with zero mean) was used

$$\xi_i \sim \text{Student}\, T(\sigma_0, \nu),$$

where parameter σ_0 determines the characteristic size of the error, and the number of degrees of freedom ν controls the presence of the aforementioned and other centroid deviations (in the limit $\nu \to \infty$, we return to the Gaussian error; $\nu = 1$ corresponds to the Cauchy distribution). In essence, σ_0 and ν, as well as T_0, are auxiliary parameters.

To complete the construction of the probabilistic model, it is sufficient to set priors on the entire set of parameters—both model parameters of the phenomenon and measurement parameters. When implementing the model in PyMC-5, uninformative uniform priors were chosen for all parameters except σ_0 and ν (for which, due to their positivity, preference was given to HalfNormal) and for H_e.

The choice of the prior for H_e allows controlling the systematic error of the reconstruction method (understood as the error in model selection) by comparing the obtained posterior distributions when H_e is fixed at different heights (practically, a normal prior with means of 90, 87.5, and 92.5 km and a standard deviation of 0.5 km was used) and when using a normal prior with standard deviations $\sigma_0 = 2.5$ and 5 km.

Figure 3 shows the sampling results for the event ELVES20190512 when the prior $p(H_e) = N(H_e|90, 2.5)$ was chosen. On the left, a one-dimensional posterior distribution $p(H_0, H_e)$ is presented, where $H_0 = z_0 + \rho^2/(2R_E)$ is the altitude of the EMP source with a correction for the spherical Earth's atmosphere ($R_E \approx 3680$ km is the mean radius of the Earth). Here, the highest density interval (HDI) is the posterior measure of the so-called "Bayesian credible interval," meaning that with a probability of 94%, the (horizontal) distance from the center of the field of view to the EMP source lies within the range of (449, 479) km. The contours on the right of Fig. 3 are drawn for HDI = 10% (inner), 20%, ..., 70%.

Due to the fact that one-dimensional distributions have a Gaussian-like shape (largely due to the volume of information conveyed in the data—almost 700 T_i estimates), the reconstruction results can also be formulated as posterior means plus/minus standard deviations: $x_0 = 381.5 \pm 6.5$, $y_0 = -263.8 \pm 4.5$, $H_0 = -10.0 \pm 8.5$, and $H_e = 88.9 \pm 1.9$ (all in km).

[4] https://mcmc-jags.sourceforge.io/.
[5] https://mc-stan.org/.
[6] https://www.pymc.io/welcome.html.

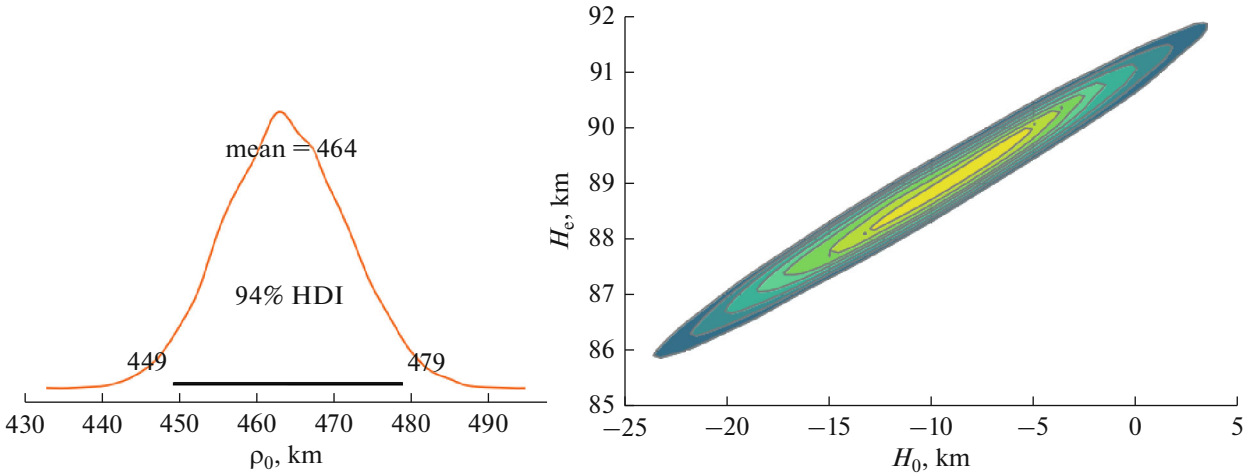

Fig. 3. Posterior distribution for the ELVES20190512 event. Left: one-dimensional distribution of distance to the center of the ring ρ_0, right: two-dimensional distribution of EMP source altitude H_0 and luminescence altitude H_e.

It is evident (see Fig. 3 on the right) that the H_0 and H_e estimates are strongly correlated; this is one of the reasons why it is quite difficult to estimate the altitude of the EMP source in this method without additional information about altitude H_e. In particular, despite the large volume of data in this event, the uncertainty of the H_0 is high (negative values of the posterior mean should not be alarming, as physically reasonable values for cloud-to-ground lightning, 1–5 km, fall within 2σ).

The posterior estimate of parameter ν is 3.3 ± 0.5, indicating that the distribution of measurement errors significantly differs from normal.

RESULTS AND DISCUSSION

It is important to emphasize that the chosen type of data, signal peak time T, provides information both about the localization of the EMP source and about the altitude at which the luminescence is generated under its influence. As a result, Bayesian inference allows making predictions for both parameters, H_0 and H_e. However, the concept of the altitude of the luminescence layer is somewhat conditional because modeling within the framework of FDTD models of the joint system of Maxwell's and Langevin's equations (see, for example, [26, 27]) indicates that the luminescence region from a typical cloud-to-ground lightning discharge has a significant height (several kilometers). Thus, the simple model proposed in this study allows estimating only a certain effective luminescence height. For a more detailed analysis of the situation, a more complex model that takes into account this "nonplanarity" of the elves is needed.

For events similar to ELVES20190512, where only a small part of the entire luminescent ring falls within the detector's field of view, the curvature of the ring relative to the detector is small (late stages of elve development). Based on kinematic data, it is difficult to localize the EMP source with high accuracy; it can be shown that, for such events, H_0 and ρ_0 are strongly correlated posteriorly.

On the other hand, Bayesian reconstruction of such events leads to strong constraints on the possible range of values for H_e (note how the standard deviation of H_e for ELVES20190512 decreased when transitioning from the prior to the posterior distribution, see also Fig. 3 on the right), if we make reasonable assumptions about parameter H_0 [28] (for example, in the form of a prior on it, by rewriting the model through H_0 instead of z_0). In particular, for two of the elves detected by Mini-EUSO, Monte Carlo sampling converges only when localizing parameter H_e, which is significantly different from the reference altitude of 90 km. For one event, the posterior distribution positions the luminescence at an effective altitude of around 80 km, for the other, closer to 95 km. The latter of these events, ELVES20200821 (see Fig. 4 on the left), along with ELVES20190512, belongs to one of the largest-scale events: at the time of detection, the diameter of the luminescent ring exceeded 800 km. In fact, this event has a complex nature and represents a sequence of rings—the second ring can be clearly seen in the figure, lagging in time from the first by approximately 100–150 μs (the uncertainty of the estimate is associated with the wide profile of the signal of the second ring). The first detection of multiple elves from space was made by the TUS detector [16, 29]. Double elves may be associated with the reflection of electromagnetic emissions from a conducting surface. In this case, the signal delay can become a reliable method for estimating H_0, weakly correlated with H_e [30].

The right side of Fig. 4 depicts another type of event—due to the large curvature of the ring, it is possible to localize the electromagnetic emission source

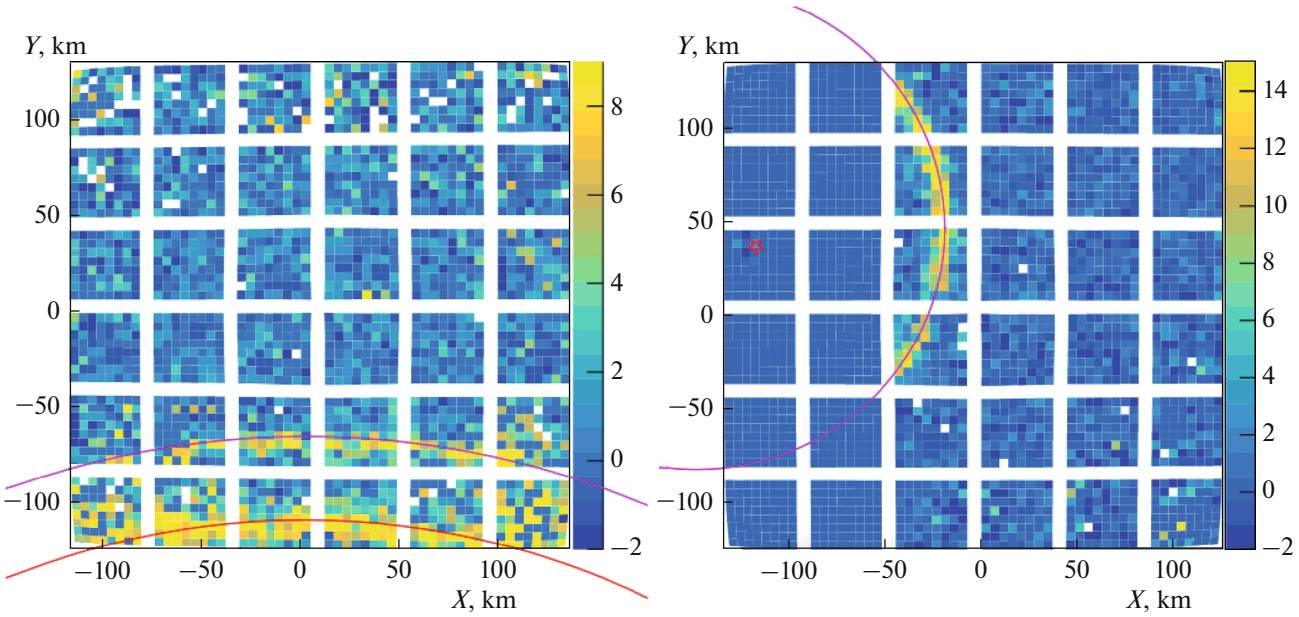

Fig. 4. Left: the ELVES20200821 event representing a sequence of rings of giant diameter. Right: the ELVES20200526 event, for which it is possible to localize the EMP source (the asterisk on the left indicates the direction to the source).

both in the horizontal plane and in altitude. For ELVES20200526 $H_0 = 3.4 \pm 5.7$ km, and the error is directly related to the uncertainty of H_e. It is worth noting that despite switching to reduced sensitivity mode for 24 MAPMTs located in the left part of the photoreceiver, the discharge area is visible, and it almost coincides with the direction to the reconstructed source.

The reconstruction of at least two elves detected by Mini-EUSO localizes the EMP source relatively high: preliminary estimates yield H_0 near 11 and 29 km (in the second case, with significant uncertainty, $\sigma_{H0} > 10$ km). Such a high location of the discharge may be surprising, as the values lie at or above the tropopause; however, EMPs from discharges at such altitudes are recorded [31, 32]. This may indicate a so-called "compact intracloud discharge" (CID), which is increasingly recognized as playing an important role in lightning initiation mechanisms [30, 33]. For such events, the dataset can be expanded to include the time of each peak in the active signal. In this case, it is expedient to formulate the probabilistic reconstruction model in two blocks. In the first block, estimate H_0 (and other parameters) is based on the time delay between peaks in those channels where such multiple peaks are reliably identified; in the second block, the model proposed in this study is used, choosing distributions obtained in the first stage as priors.

In this study, the probabilistic model includes only the localization of the EMP source but not its orientation. For this reason, selecting only the peak time of the active channel as data was sufficient. In reality, as can be easily verified, the signal amplitude varies along the ring, which is apparently related to the nonvertical orientation of the effective discharge dipole. If data D are supplemented with information not only about the peak position(s) in time T but also its (their) magnitude A (amplitude or total signal), an extended model can be formulated, in which the unknown parameters will additionally include the angles of the dipole orientation. Currently, work is underway to perform a detailed analysis of the active signals of all elves recorded by Mini-EUSO, with preliminary results available in [22]. This work on identifying "signal morphology" will help clarify which of the multipeak events are due to ground reflection and which are manifestations of the complex structure of the discharge current pulse [27, 30].

CONCLUSIONS

Orbital "photography" of elves is a way to penetrate inside a storm cloud. This dynamic imprint of an electrical discharge contains information about a complex of phenomena associated with storm activity—both during the lightning discharge itself and during the period immediately preceding it, i.e., during lightning initiation.

The UV Atmosphere detector (Mini-EUSO), observing the atmosphere from the *ISS*, has obtained detailed data on more than three dozen elve-like events, partially or fully captured in its field of view. The scale of the recorded events is impressive: taking it into account that, at the moment, only a fraction of the detector's data has been processed and its operation continues, it is quite expected to discover elves with

diameters of up to 1000 km in the future. The possibility of detecting elves of such large sizes has arisen due to the Mini-EUSO's relatively high sensitivity.

In this study, a probabilistic reconstruction model of elves has been developed, implemented using probabilistic programming methods in PyMC. Using several examples of events recorded by Mini-EUSO, the application of Bayesian reconstruction of the position of the electrical discharge generating the elve and the height of the glow has been demonstrated. Paths for further improving the model have been outlined, allowing for the estimation of the discharge orientation and current pulse structure, as well as taking into account additional information when the signal reflects off the Earth's surface.

ACKNOWLEDGMENTS

This study was supported by the State Corporation Roscosmos and the JEM-EUSO collaboration. The paper was prepared based on research carried out in the "UV Atmosphere" experiment on the Russian segment of the *ISS*.

FUNDING

This work was supported by ongoing institutional funding. No additional grants to carry out or direct this particular research were obtained.

CONFLICT OF INTEREST

The authors of this work declare that they have no conflicts of interest.

REFERENCES

1. Casolino, M., Klimov, P., and Piotrowski, L., Observation of ultra high energy cosmic rays from space: Status and perspectives, Progress of Theoretical and Experimental Physics, 2017, no. 12, p. 12A107. https://doi.org/10.1093/ptep/ptx169
2. Capel, F., Belov, A., Casolino, M., et al., Mini-EUSO: A high resolution detector for the study of terrestrial and cosmic UV emission from the international space station, *Adv. Space Res.,* 2018, vol. 62, no. 10, pp. 2954–2965. https://doi.org/10.1016/j.asr.2017.08.030
3. Bacholle, S., Barrillon, P., Battisti, M., et al., Mini-EUSO mission to study Earth UV emissions on board the ISS, *Astrophys. J. Suppl. Ser.,* 2021, vol. 253, no. 2, p. 36. https://doi.org/10.3847/1538-4365/abd93d
4. Capel, F., Belov, A., Cambiè, G., et al., Mini-EUSO data acquisition and control software, *J. Astron. Telesc., Instrum. Syst.,* 2019, vol. 5, no. 4. https://doi.org/10.1117/1.JATIS.5.4.044009
5. Casolino, M., Barghini, D., Battisti, M., et al., Observation of night-time emissions of the earth in the near UV range from the international space station with the Mini-EUSO detector, *Remote Sens. Environ.,* 2023, vol. 284, p. 113336. https://doi.org/10.1016/j.rse.2022.113336
6. Belov, A., Bertaina, M., Capel, F., et al., The integration and testing of the mini-EUSO multi-level trigger system, *Adv. Space Res.,* 2018, vol. 62, no. 10, pp. 2966–2976. https://doi.org/10.1016/j.asr.2017.10.044
7. Bertaina, M., Barghini, D., Battisti, M., et al., Description and performance results of the trigger logic of TUS and mini-EUSO to search for ultra-high energy cosmic rays from space, *Nucl. Instrum. Methods Phys. Res. A,* 2023, vol. 1045, p. 167601. https://doi.org/10.1016/j.nima.2022.167601
8. JEM-EUSO Collaboration, Science of atmospheric phenomena with JEM-EUSO, *Exp. Astron.,* 2015, vol. 40, pp. 239–251. https://doi.org/10.1007/s10686-014-9431-0
9. Marcelli, L., Arnone, E., Barghini, M., et al., Observation of ELVES with mini-EUSO telescope on board the International Space Station, *Proc. 37th International Cosmic Ray Conference,* 2021. https://doi.org/10.22323/1.395.0367
10. Inan, U.S., Bell, T.F., and Rodriguez, J.V., Heating and ionization of the lower ionosphere by lightning, *Geophys. Res. Lett.,* 1991, vol. 18, no. 4, pp. 705–708. https://doi.org/10.1029/91GL00364
11. Fukunishi, H., Takahashi, Y., Kubota, M., et al., Elves: Lightning-induced transient luminous events in the lower ionosphere, *Geophys. Res. Lett.,* 1996, vol. 23, no. 16, pp. 2157–2160.
12. Chang, S.C., Kuo, C.L., Lee, L.J., et al., ISUAL far-ultraviolet events, elves, and lightning current, *J. Geophys. Res.: Space Phys.,* 2010, vol. 115, no. A7. https://doi.org/10.1029/2009JA014861
13. Newsome, R.T. and Inan, U.S., Free-running ground-based photometric array imaging of transient luminous events, *J. Geophys. Res.: Space Phys.,* 2010, vol. 115, no. A7. https://doi.org/10.1029/2009JA014834
14. Boeck, W.L., Vaughan, O., Jr., Blakeslee, R., et al., Lightning induced brightening in the airglow layer, *Geophys. Res. Lett.,* 1992, vol. 19, no. 2, pp. 99–102. https://doi.org/10.1029/91GL03168
15. Chern, J.L., Hsu, R.R., Su, H.T., et al., Global survey of upper atmospheric transient luminous events on the ROCSAT-2 satellite, *J. Atmos. Sol.-Terr. Phys.,* 2003, vol. 65, no. 5, pp. 647–659. https://doi.org/10.1016/S1364-6826(02)00317-6
16. Klimov, P., Khrenov, B., Kaznacheeva, M., et al., Remote sensing of the atmosphere by the ultraviolet detector TUS onboard the Lomonosov satellite, *Remote Sens.,* 2019, vol. 11, no. 20, p. 2449. https://doi.org/10.3390/rs11202449
17. Klimov, P.A., Sharakin, S.A., and Kaznacheeva, M.A., Double elves measured by the TUS space detector, *Proc. Int. Conf. Atmosphere, Ionosphere, Safety,* 2020, pp. 137–140.
18. Chen, A.B., Kuo, C.L., Lee, Y.J., et al., Global distributions and occurrence rates of transient luminous events, *J. Geophys. Res.: Space Phys.,* 2008, vol. 113, no. A8. https://doi.org/10.1029/2008JA013101

19. Adashko, J.G. and Gurevich, A., *Nonlinear Phenomena in the Ionosphere,* Physics and Chemistry in Space, Berlin: Springer, 1978. https://doi.org/10.1007/978-3-642-87649-3
20. Taranenko, Y.N., Inan, U.S., and Bell, T.F., Interaction with the lower ionosphere of electromagnetic pulses from lightning: Heating, attachment, and ionization, *Geophys. Res. Lett.,* 1993, vol. 20, no. 15, pp. 1539–1542.
21. Piotrowski, L.W. *for the JEM-EUSO Collaboration*, A search for Elves in Mini-EUSO data using CNN-based one-class classifier, *Proc. Sci.,* 2023, vol. 444, p. 333. https://doi.org/10.22323/1.444.0333
22. Romoli, G. *for the JEM-EUSO Collaboration*, Study of multiple ring ELVES with the Mini-EUSO telescope on-board the International Space Station, *Proc. Sci.,* 2023, vol. 444, p. 223. https://doi.org/10.22323/1.444.0223
23. Jaynes, E.T., *Probability Theory: The Logic of Science,* Cambridge University Press, 2003.
24. Sivia, D.S. and Skilling, J., *Data Analysis: A Bayesian Tutorial,* Oxford Science Publications, Oxford University Press, 2006.
25. Martin, O., Bayesian analysis with Python: Introduction to statistical modeling and probabilistic programming using PyMC3 and ArviZ, Packt Publishing Ltd., 2018.
26. Inan, U.S., Sampson, W.A., and Taranenko, Y.N., Space-time structure of optical flashes and ionization changes produced by lighting-EMP, *Geophys. Res. Lett.,* 1996, vol. 23, no. 2, pp. 133–136. https://doi.org/10.1029/95GL03816
27. Marshall, R.A., An improved model of the lightning electromagnetic field interaction with the D-region ionosphere, *J. Geophys. Res.: Space Phys.,* 2012, vol. 117, no. A3. https://doi.org/10.1029/2011JA017408
28. Uman, M.A., *Lightning,* Courier Corporation, 2012.
29. Kaznacheeva, M.A., Klimov, P.A., and Khrenov, B.A., Transient UV background when registering EASes with the TUS orbital detector, *Bull. Russ. Acad. Sci.: Phys.,* 2019, vol. 83, pp. 1024–1027. https://doi.org/10.3103/S1062873819080173
30. Marshall, R.A., Da Silva, C.L., and Pasko, V.P., Elve doublets and compact intracloud discharges, *Geophys. Res. Lett.,* 2015, vol. 42, no. 14, pp. 6112–6119. https://doi.org/10.3103/S1062873819080173
31. Smith, D.A., Heavner, M.J., Jacobson, A.R., et al., A method for determining intracloud lightning and ionospheric heights from VLF/LF electric field records, *Radio Sci.,* 2004, vol. 39, no. 1, pp. 1–11. https://doi.org/10.1029/2002RS002790
32. Nag, A., Rakov, V.A., and Cramer, J.A., Remote measurements of currents in cloud lightning discharges, *IEEE Trans. Electromagn. Compat.,* 2010, vol. 53, no. 2, pp. 407–413.
33. Kostinskiy, A.Y., Marshall, T.C., and Stolzenburg, M., The mechanism of the origin and development of lightning from initiating event to initial breakdown pulses (v. 2), *J. Geophys. Res.: Atmos.,* 2020, vol. 125, no. 22, p. e2020JD033191. https://doi.org/10.1029/2020JD033191

Translated by M. Chubarova